

Imaging the Interaction between Planets and Young Disks with the ngVLA

Sarah Harter¹, Luca Ricci¹, Shanjia Zhang², and Zhaohuan Zhu²

¹CSU Northridge

²Univeristy of Nevada Las Vegas

November 26, 2022

Abstract

The recent discovery of thousands of protoplanetary disks and exoplanets has revealed that planet formation is a very efficient process in nature. There have been several theories to describe the many steps along this process, but it remains difficult to discover planets surrounding young stars. Thanks to its unprecedented angular resolution and sensitivity at radio wavelengths where the emission from the circumstellar material is optically thin, the future ngVLA telescope has the potential to transform our understanding of planet formation. In this presentation I will highlight the unprecedented imaging capabilities of the ngVLA using theoretical models of protoplanetary disks with varying planet and stellar masses. These theoretical models showcase the temporal evolution of the separation of gas and dust that in turn forms gaps and rings within the protoplanetary disk. These images will help shed light on how planets interact with disks and young stars, as well as on the properties of forming exoplanetary systems. Our findings suggest that the ngVLA would be capable of detecting the signatures in the disk of terrestrial planets at few astronomical units from the host star.

Imaging the Interaction between Young Planets and Disks with the ngVLA



Sarah Harter¹, Luca Ricci¹, Zhaohuan Zhu², Shangjia Zhang²

¹California State University Northridge, CA ²University of Las Vegas, Las Vegas, NV

Introduction

Protoplanetary disks are the cradles of planets. Disks can be spatially resolved at mm-radio wavelengths using radio interferometers. The Next Generation Very Large Array is a potential future radio interferometer (Fig 1) that would improve on the capabilities of current Very Large Array by factors 10-100 (Fig 2). The research conducted here is a case study to quantify the potential of the ngVLA to image protoplanetary disks at < 0.1 - 1au resolution and improve our understanding of planetary formation.

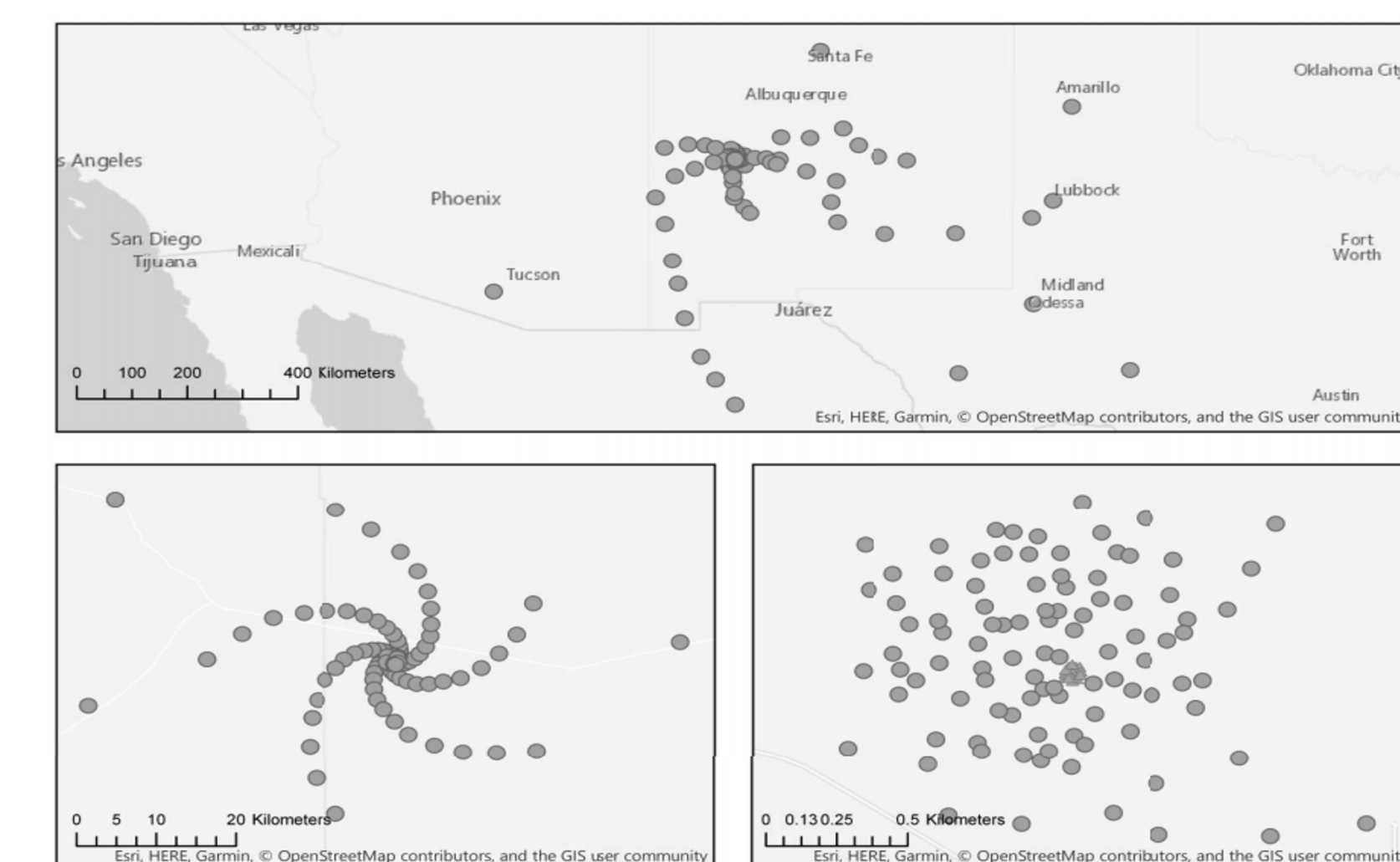


Fig 1. The positions of the ngVLA antennas according to its current design.

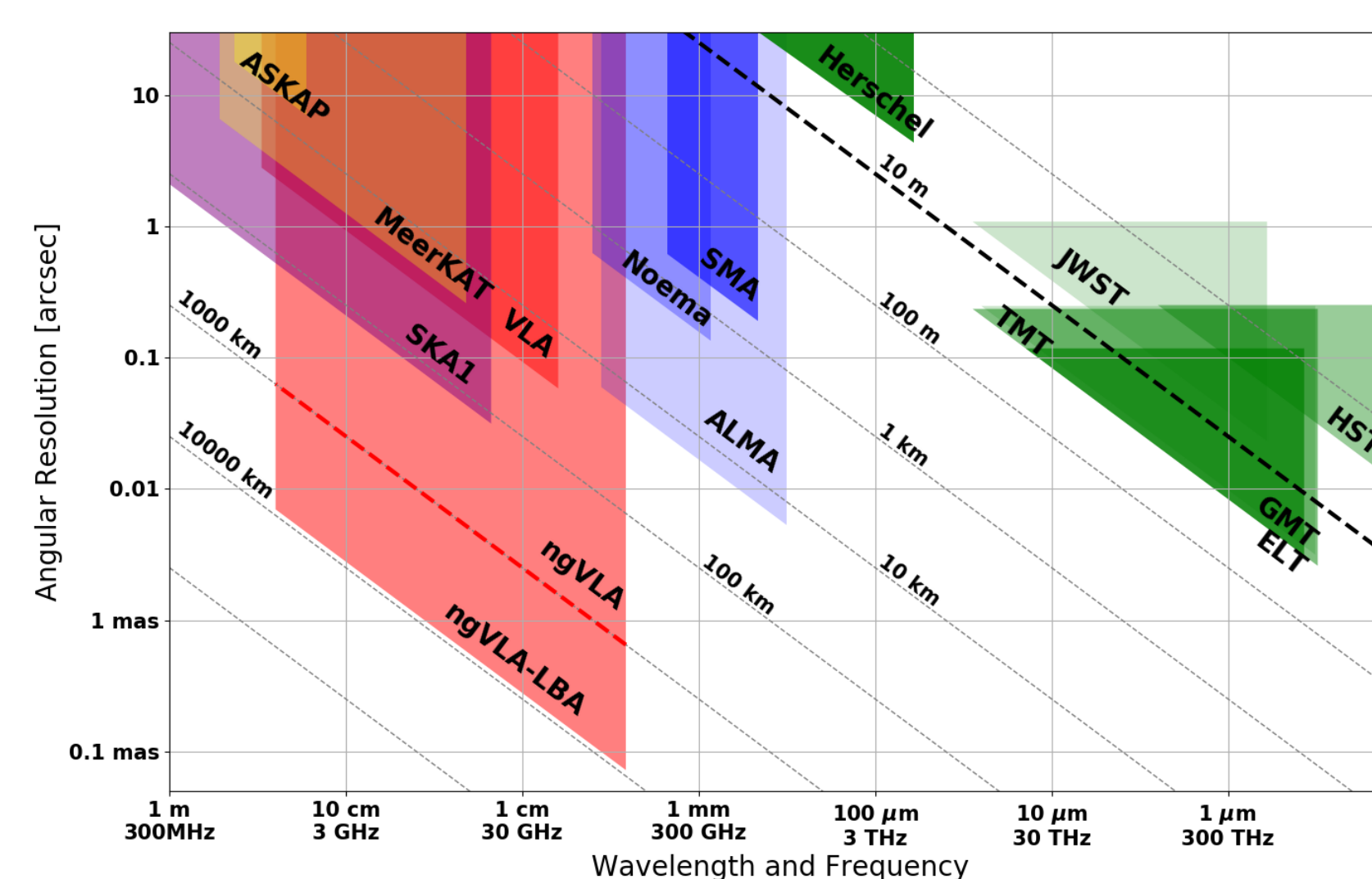


Fig. 2 The capabilities of the ngVLA compared to other radio interferometers. The ngVLA can operate at wavelengths from 2.6 mm up to 25 cm

Methodology

We are producing disk models with planets to quantify the potential of the ngVLA to image these systems at high resolution. The model for these simulations were created using the version of the FARGO code called Dusty FARGO-ADSG for 2-D hydrodynamical planet-disk simulations (Masset 2000; Baruteau & Zhu 2016). This model accounts for the dynamics of gas and dust in a disc with an embedded planet. This code can calculate the gravitational interaction between gas and dust with the planet and the aerodynamical coupling between gas and dust.

We used RADMC-3D (Dullemond 2012) to generate synthetic images for the dust continuum from this model at wavelengths 3 mm and 1 cm. In order to predict the results of future observations with the ngVLA we used those model images as input for CASA tasks such as simobserve and clean. The simobserve task was used to derive the visibility datasets from the model image accounting for the proper sampling of the interferometric (u,v) space with the ngVLA, while clean was used for the imaging of the visibilities, using the same method described in Ricci et al. (2018).

Results

In our models, we investigated two cases of planet mass with $1 M_{\oplus}/M_{\odot}$ and $10 M_{\oplus}/M_{\odot}$. These are corresponding to an Earth-mass planet and 10 M_{\oplus} -mass Super Earth around a solar-mass star, or a Mars-mass planet and Earth-mass planet around a 0.1 M_{\odot} M-type young star, respectively. The case for the $1 M_{\oplus}/M_{\odot}$ simulation was run up to 7000 planet orbits with the planet at 2 or 3 au from the host star. In the case for $10 M_{\oplus}/M_{\odot}$, the simulation was run up to 5000 planet orbits with the planet at 1 or 3 au from the host star. The synthetic maps for the dust continuum emission of the models were derived at wavelengths of 1.25mm, 3mm, 7mm and 1cm.

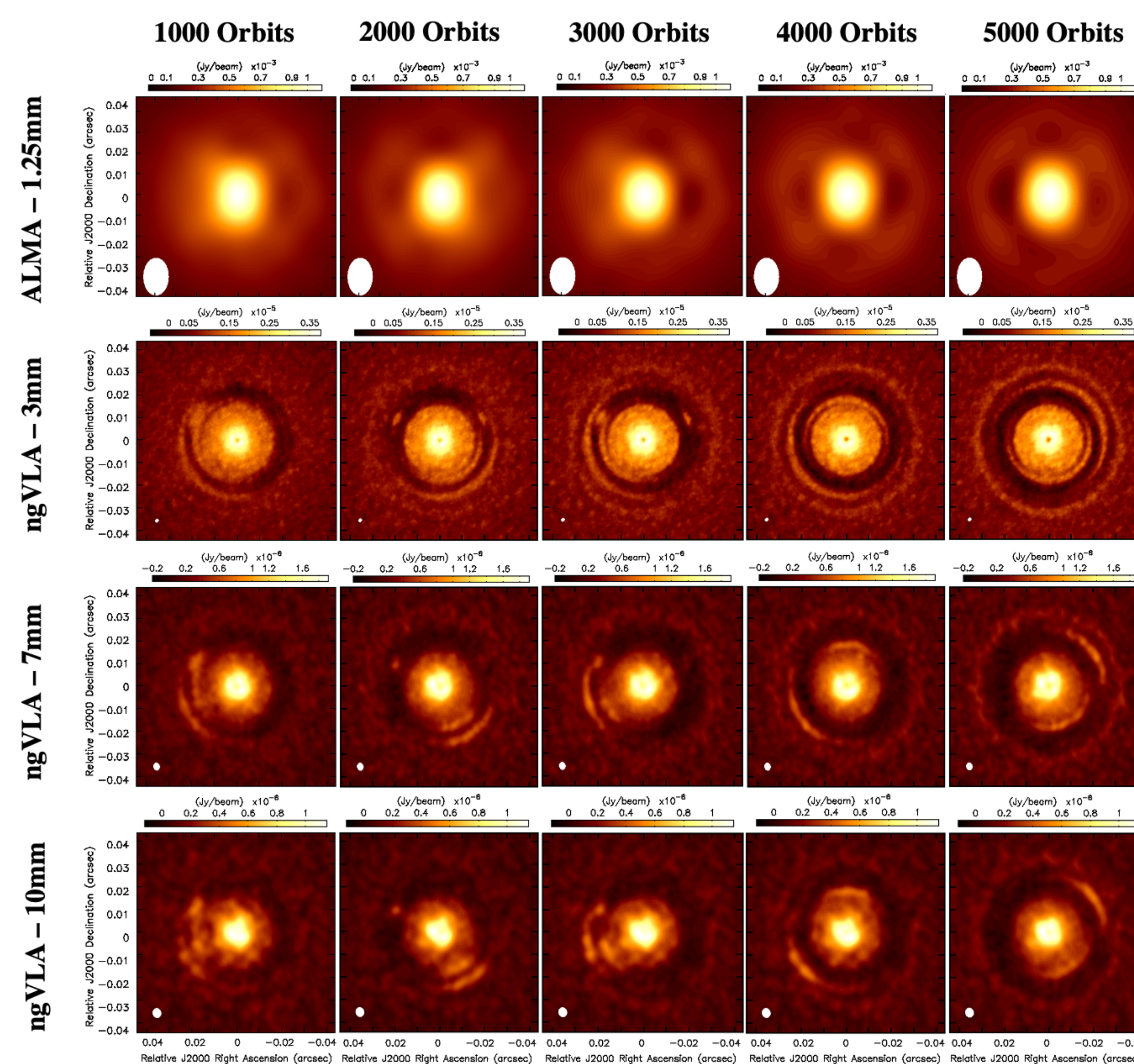


Fig 3. ALMA and ngVLA simulated observations for the dust continuum emission at 1.25 mm (ALMA), 3 mm, 7 mm, and 10 mm (ngVLA) for disk models with a planet with planet-mass ratio of $10 M_{\oplus}/M_{\odot}$ at 3 au from the host star, $L^* = 10$, and a surface gas density of 300 g/cm^2 from the host star. Each row represents the specific orbit from left to right of 1000, 2000, 3000, 4000, and 5000 orbits. The resulting synthesized beam has a FWHM = 18 mas (2.5 au) \times 12 mas (1.7 au) for 1.25 mm, 1.7 mas (0.23 au) \times 1.3 mas (0.19 au) for 3 mm wavelength, 3.4 mas ($.47 \text{ au}$) \times 2.7 mas ($.38 \text{ au}$) for 7 mm wavelength, and 4.2 mas ($.59 \text{ au}$) \times 3.7 mas ($.52 \text{ au}$) for 10 mm wavelength at the assumed distance of 140pc for our disk model.

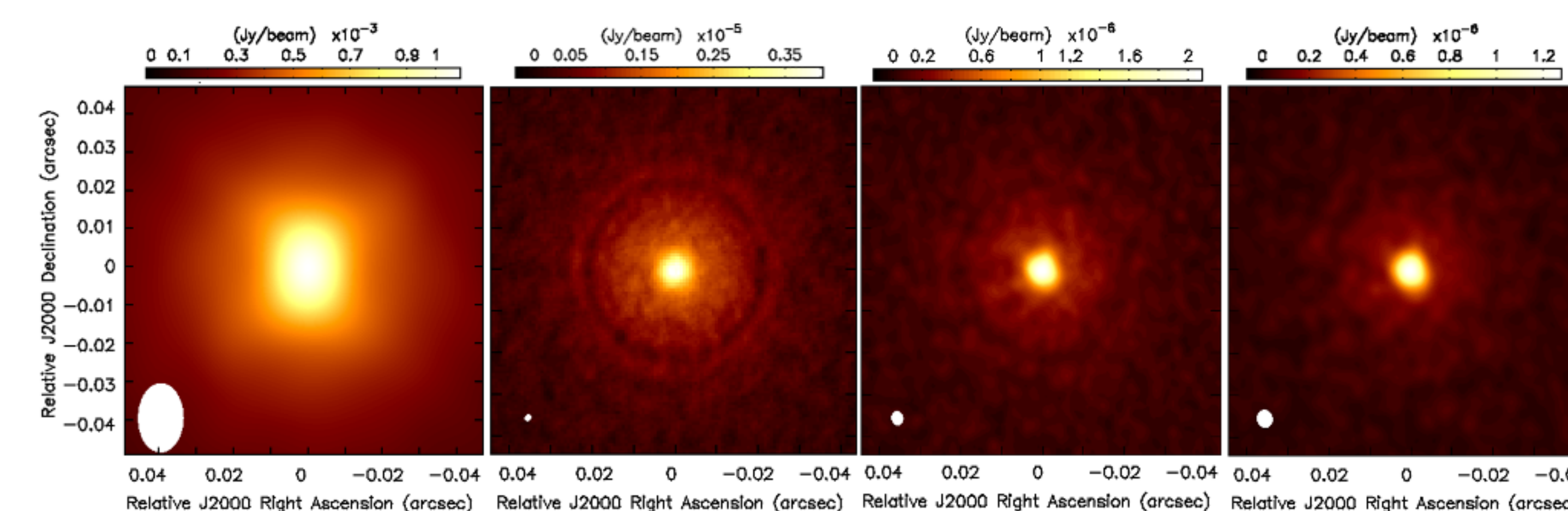


Fig 4. ALMA and ngVLA simulated observations for the dust continuum emission at 1.25 mm (ALMA), 3 mm, 7 mm, and 10 mm (ngVLA) for disk models with a planet with planet-mass ratio of $1 M_{\oplus}/M_{\odot}$ at 3 au from the host star, $L^* = 10$, and a surface gas density of 300 g/cm^2 from the host star at 7000 orbits. The resulting synthesized beam has a FWHM = 18 mas (2.5 au) \times 12 mas (1.7 au) for 1.25 mm, 1.7 mas (0.23 au) \times 1.3 mas (0.19 au) for 3 mm wavelength, 3.4 mas ($.47 \text{ au}$) \times 2.7 mas ($.38 \text{ au}$) for 7 mm wavelength, and 4.2 mas ($.59 \text{ au}$) \times 3.7 mas ($.52 \text{ au}$) for 10 mm wavelength at the assumed distance of 140pc for our disk model.

Due to the low viscosity that is present in the disk, the planet can produce multiple rings in the gas distribution (Dong et al. 2017). For larger planet masses, the difference between the gas and dust gaps is more obvious due to the gas pressure which makes the radial drift on a particle more effective. In the case of these simulations with a gap created by a planet at 3 au, dust is then pulled to the inner and outer edges of the gap, due to the pressure gradient at the gap edges. A gap in the dust component is then more obvious than in gas. This effect is stronger for larger dust grain sizes.

Figure 3 showcases the results of the ALMA and ngVLA observations for models of the $10 M_{\oplus}/M_{\odot}$ planet. In these simulations the disk is moving in a counter-clockwise motion, which causes most of the material is trapped behind the planet. In the cases of these super-Earth masses at 3 au, the gap structure is detected by all four wavelengths shown, i.e. 1.25 mm (ALMA), 3mm, 7mm, and 10mm (ngVLA). With the higher angular resolution and more efficient dust trapping of larger particles, the asymmetries are better resolved with the ngVLA at 3 mm than with ALMA.

In the case of the $10 M_{\oplus}/M_{\odot}$ planet, the ngVLA at all wavelengths has the ability to detect corotating material with the planet at the specified orbital radius. This feature is also visible in the azimuthally average radial profile of the surface density, found in Figure 3, of both the gas and dust.

In the case of $1 M_{\oplus}/M_{\odot}$ planet at 3 au, the gap is only detected by longer wavelengths of 3mm, 7mm, and 10mm (ngVLA). The difference between the gas and dust gaps is more pronounced for more massive planets. With a significantly lower planet mass, these simulations do not produce any significant sub-structures that can be observed. It can also be seen that the gap radial width shrinks, and ngVLA observations are the only ones that can spatially resolve the gap. The gaps for the latter wavelengths, 7mm and 10mm are only visible at the highest number of orbits, 7000. For 3 mm wavelengths, the gap is visible as early as 4000 orbits. These observations do not display any of the previously resolved substructures such as the long arcs and asymmetries as in the case of the larger planet. In figure 4, it can be seen with the lower-mass planet that the gas density is not as widely distributed nearing the gap, but has a dip where the planet is present, and dust trappings at the edge due to radial drift.

Conclusion and Future Perspectives

Our work shows that the ngVLA with its current design would be capable of imaging disk structures due to the interaction with an embedded planets in the disk. By constraining the morphology of these structures we would be able to locate the planet in the disk and get information on its mass. Being able to know more about protoplanetary disks allow us to learn more about the formation of solar systems, planets, as well as planetesimals. We plan on applying this method to explain the results of observations of real disks with ALMA and to predict the results of future observations of the same systems with the ngVLA.

References

- [1] Baruteau, C., & Zhu, Z. 2016, MNRAS, 458, 3927
- [2] Dong R., Li S., Chiang E. and Li H. 2017 ApJ 843 127
- [3] Dullemond C. P., 2012, RADMC-3D: A multi-purpose radiative transfer tool (ascl:1202.015)
- [4] Murphy E., ed. 2018, Science with a Next Generation Very Large Array ASP Conf. Ser. Vol. 517.
- [5] Masset, F. 2000, A&AS, 141, 165
- [6] Ricci, L., Liu, S.-F., Isella, A., & Li, H. 2018, ApJ, 853, 110
- [7] Zhang, S., Zhu, Z., Huang, J., et al. 2018, ApJL, 869, L47

Sarah Harter
B.Sc. Astrophysics
Department of Physics and Astronomy
California State University, Northridge
18111 Nordhoff St. Northridge, CA 91330
sarah.harter.584@my.csun.edu